Long-Distance Entanglement Purification for Quantum Communication

Xiao-Min Hu,[1,4] Cen-Xiao Huang,[1,4] Yu-Bo Sheng,[2,3,5,*] Lan Zhou,[2,3,5] Bi-Heng Liu,[1,4,†] Yu Guo,[1,4] Chao Zhang,[1,4] Wen-Bo Xing,[1,4] Yun-Feng Huang,[1,4] Chuan-Feng Li,[1,4,‡] and Guang-Can Guo[1,2,4,5]

[1]*CAS Key Laboratory of Quantum Information, University of Science and Technology of China, Hefei 230026, People's Republic of China*

[2]*Institute of Quantum Information and Technology, Nanjing University of Posts and Telecommunications, Nanjing 210003, People's Republic of China*

[3]*School of Science, Nanjing University of Posts and Telecommunications, Nanjing 210003, People's Republic of China*

[4]*CAS Center For Excellence in Quantum Information and Quantum Physics, University of Science and Technology of China, Hefei 230026, People's Republic of China*

[5]*Key Lab of Broadband Wireless Communication and Sensor Network Technology, Nanjing University of Posts and Telecommunications, Ministry of Education, Nanjing 210003, People's Republic of China*

(Received 1 August 2020; accepted 3 December 2020; published 8 January 2021)

High-quality long-distance entanglement is essential for both quantum communication and scalable quantum networks. Entanglement purification is to distill high-quality entanglement from low-quality entanglement in a noisy environment and it plays a key role in quantum repeaters. The previous significant entanglement purification experiments require two pairs of low-quality entangled states and were demonstrated in tabletop. Here we propose and report a high-efficiency and long-distance entanglement purification using only one pair of hyperentangled state. We also demonstrate its practical application in entanglement-based quantum key distribution (QKD). One pair of polarization spatial-mode hyperentanglement was distributed over 11 km multicore fiber (noisy channel). After purification, the fidelity of polarization entanglement arises from 0.771 to 0.887 and the effective key rate in entanglement-based QKD increases from 0 to 0.332. The values of Clauser-Horne-Shimony-Holt inequality of polarization entanglement arises from 1.829 to 2.128. Moreover, by using one pair of hyperentanglement and deterministic controlled-NOT gates, the total purification efficiency can be estimated as 6.6×10^3 times than the experiment using two pairs of entangled states with spontaneous parametric down-conversion sources. Our results offer the potential to be implemented as part of a full quantum repeater and large-scale quantum network.

DOI: 10.1103/PhysRevLett.126.010503

Quantum entanglement [1] plays an essential role in both quantum communication [2–5] and scalable quantum networks [6]. However, the unavoidable environmental noise degrades entanglement quality. Entanglement purification is a powerful tool to distill high-quality entanglement from low-quality entanglement ensembles [7,8] and is the heart of quantum repeaters [9]. Several significant entanglement purification experiments using photons [10,11], atoms [12], and electron-spin qubits [13] were reported. These experiments were all tabletop and did not distribute entanglement over a long distance. Moreover, these experiments based on Ref. [7] were low efficiency for they require two copies of low-quality entangled states and consume at least one pair of low-quality entangled states even if the purification is successful. In optical systems, a spontaneous parametric down-conversion (SPDC) source is commonly used to generate entangled states. The probabilistic nature of SPDC makes it still challenging to generate two clean pairs of entangled states simultaneously because of double-pair emission noise [11].

Hyperentanglement [14], simultaneous entanglement with more than one degree of freedom (d.o.f.), is more powerful and can be used to increase the channel capacity [15,16]. Hyperentanglement also fulfills quantum teleportation of a single photon with multiple d.o.f. [17–19]. The distribution of hyperentanglement were also reported [20,21]. Some entanglement purification protocols (EPPs) assisted by spatial-mode d.o.f. have been proposed [22–24]. Such deterministic entanglement purification usually requires the spatial or other entanglement to be more robust. The fidelity of purified polarization entanglement equals the fidelity of spatial entanglement, and this is essentially the transformation from spatial entanglement to polarization entanglement.

Here we propose and report the first high-efficiency long-distance polarization entanglement purification using only one pair of hyperentanglements. We also demonstrate its practical application in entanglement-based quantum key distribution (QKD) [25]. We show that the EPP using two copies [7] and subsequent experiments [10–13] is not

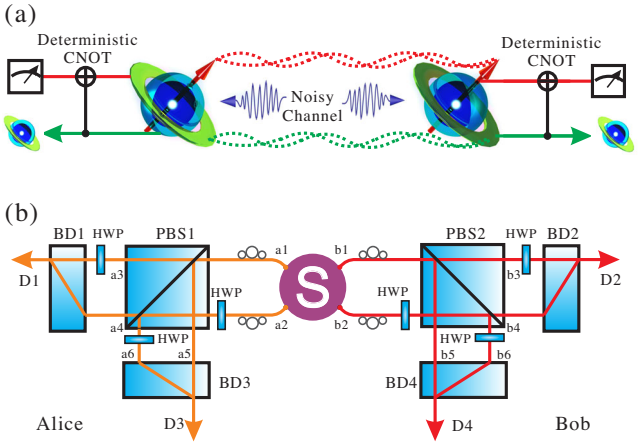

FIG. 1. Protocol of entanglement purification using hyperentanglement. (a) General protocol of long-distance entanglement purification using hyperentanglement. After long-distance distribution, deterministic CNOT operations are performed between different degrees of freedom of single particles. Then the target qubits (encoded in 1 degree of freedom) are measured. If we only keep the same measurement results, then the entanglement encoded in the other degree of freedom (control qubits) is purified. (b) Purification protocol based on polarization-spatial-mode hyperentanglement. The hyperentangled state $|\Phi^+\rangle_{ab} \otimes |\phi^+\rangle_{ab}$ is first generated by the entanglement source (S) and then distributed to Alice and Bob in the channel (a_1b_1, a_2b_2). After suffering from the channel noise, the entanglement purification is performed. The entanglement purification operation uses a half-wave plate (HWP, set at 45°) and a polarizing beam splitter (PBS, which transmits the H-polarized photon and reflects the V-polarized photon). This essentially acts as a CNOT gate with a success probability of 100% between the polarization (target qubits) and spatial-mode (control qubits) degree of freedom. After PBS1 and PBS2, we convert the spatial mode to polarization. Thus, we can verify its success by selecting the cases in which the two photons are in the output-mode state D_1D_2 or D_3D_4. The beam displacer (BD) can couple H- and V-polarized components from different spatial modes.

necessary and polarization entanglement can be purified using entanglement in other d.o.f. Moreover, the double-pair emission noise using SPDC source is removed automatically and the purification efficiency can be greatly increased in a second time. A general protocol is shown in Fig. 1(a). In our experiment, we use hyperentanglement encoded on polarization and spatial modes. As shown in Fig. 1(b), a hyperentangled state $|\phi\rangle = |\Phi^+\rangle_{ab} \otimes |\phi^+\rangle_{ab}$ is distributed to Alice and Bob. $|\Phi^+\rangle_{ab}$ is one of the polarization Bell states $|\Phi^\pm\rangle_{ab} = (1/\sqrt{2})(|H\rangle_a|H\rangle_b \pm |V\rangle_a|V\rangle_b)$, and $|\Psi^\pm\rangle_{ab} = (1/\sqrt{2})(|H\rangle_a|V\rangle_b \pm |V\rangle_a|H\rangle_b)$. $|\phi^+\rangle_{ab}$ is one of the spatial-mode Bell states $|\phi^\pm\rangle_{ab} = (1/\sqrt{2})(|a_1\rangle|b_1\rangle \pm |a_2\rangle|b_2\rangle)$, and $|\psi^\pm\rangle_{ab} = (1/\sqrt{2})(|a_1\rangle|b_2\rangle \pm |a_2\rangle|b_1\rangle)$, where $H(V)$ denotes horizontal (vertical) polarization, and a_1, b_1, a_2, and b_2 are the spatial modes. The noise channel makes the hyperentangled state become a mixed state as $\rho_{ab} = \rho^P_{ab} \otimes \rho^S_{ab}$ with

$$\rho^P_{ab} = F_1|\Phi^+\rangle_{ab}\langle\Phi^+| + (1-F_1)|\Psi^+\rangle_{ab}\langle\Psi^+| \quad (1)$$

and

$$\rho^S_{ab} = F_2|\phi^+\rangle_{ab}\langle\phi^+| + (1-F_2)|\psi^+\rangle_{ab}\langle\psi^+|. \quad (2)$$

The principle of purification is to select the cases in which the photons are in the output modes D_1D_2 or D_3D_4 (see Supplemental Material [26]) and we can obtain a new mixed state

$$\rho'_{ab} = F'|\Phi^+\rangle_{ab}\langle\Phi^+| + (1-F')|\Psi^+\rangle_{ab}\langle\Psi^+|. \quad (3)$$

Here $F' = \{[F_1F_2]/[F_1F_2 + (1-F_1)(1-F_2)]\}$. If $F_1 > \frac{1}{2}$ and $F_2 > \frac{1}{2}$, we can obtain $F' > F_1$ and $F' > F_2$.

To demonstrate the purification, we first generated one pair of hyperentangled state. As shown in Fig. 2(a), a continuous-wave (c.w.) laser operated at 775 nm is separated into two spatial modes (p_1 and p_2) by a beam displacer and then injected to a polarization Sagnac interferometer to generate polarization-entangled photon pair [31] in each spatial mode [16,21,32]. Noticed that we use a c.w. laser; the final state is the superposition of the states in each mode. Thus, we can generate the hyperentanglement $|\phi\rangle = |\Phi^+\rangle_{ab} \otimes |\phi^+\rangle_{ab}$ by tuning the relative phase between the two spatial modes. We used 200 mW pumped light to excite 2400 photon pairs/s. The coincidence efficiency of the entangled source is 18%. To show the performance of entanglement purification in the noisy channel, we distributed the hyperentangled state over an 11 km multicore fiber (MCF) [21,33–35]. The difficulty of long-distance distribution of polarization and spatial-mode hyperentanglement is maintaining the coherence and phase stability between different paths. The MCF provides an ideal platform for distributing spatial-mode states over a long distance. The distance between the nearest two cores of the MCF is very small (approximate 41.5 μm), and the noises of different paths are very close, so it can maintain coherence [21,33–35]. However, there are still some other difficulties, such as the polarization-maintaining and group delay mismatch. To overcome these obstacles, we used a phase-locking system to ensure the effective distribution of hyperentanglement [21,26]. In Fig. 2(b), the hyperentangled state $|\phi\rangle$ was distributed over 11 km in the MCF. During distribution, a small bit flip (BF) error ($|\Psi^+\rangle_{ab}$ and $|\psi^+\rangle_{ab}$) and small phase flip (PF) error ($|\Phi^-\rangle_{ab}$ and $|\phi^-\rangle_{ab}$) were introduced by the fiber noise environment. The fidelities of the hyperentangled state in the polarization and spatial modes were $F_P = 0.961 \pm 0.001$ and $F_S = 0.952 \pm 0.001$, respectively. Here, we use superconducting single photon detectors to detect each photon, the efficiency is 80%, and the dark count rate is approximate 300 Hz. Including all the losses, the coincidence efficiency was ~8.1%, and the coincident count rate was 600 Hz.

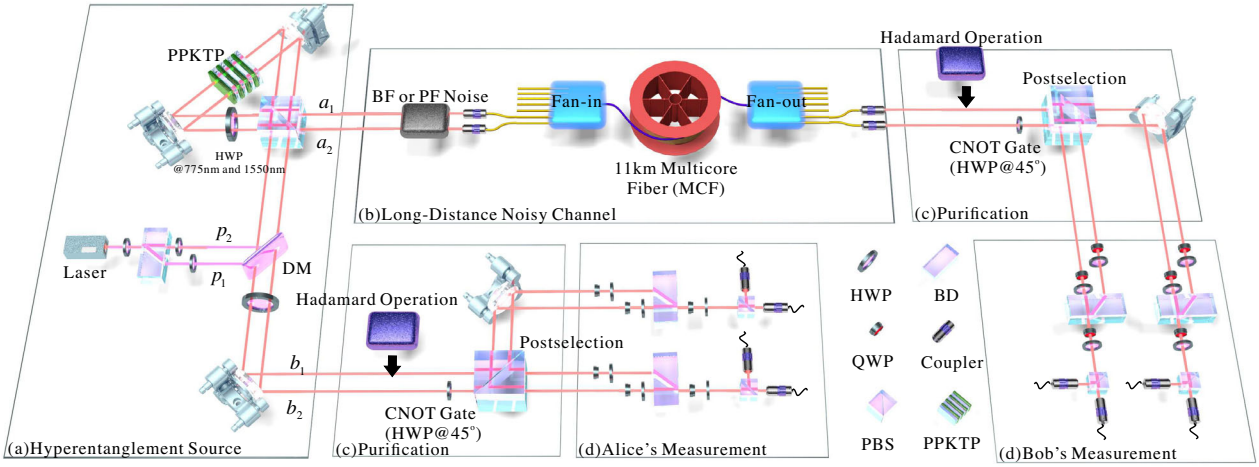

FIG. 2. Experimental setup. (a) Preparation of hyperentangled state. The pump light beam is separated into two spatial modes by the BD. These two beams are injected into a Sagnac interferometer to pump a type-II cut periodically poled potassium titanyl phosphate (PPKTP) crystal ($1 \times 7 \times 10$) mm and generate the two-photon polarization entanglement $1/\sqrt{2}(|HV\rangle + |VH\rangle)$ in each spatial mode. After HWP1 (set at 45°), the hyperentangled state $|\Phi^+\rangle_{ab} \otimes |\phi^+\rangle_{ab} = 1/\sqrt{2}(|HH\rangle + |VV\rangle) \otimes 1/\sqrt{2}(|a_1 b_1\rangle + |a_2 b_2\rangle)$ is generated. (b) Quantum noisy channel. This channel is divided into two parts. The first part is a controllable spatial mode and polarization BF or PF loading noise setup. The other part is an 11 km MCF. (c) Purification process. This process is also divided into two steps. The first step is a CNOT gate between the spatial mode and polarization d.o.f. The setup consists of a HWP (set at 45°) placed on spatial modes a_2 and b_2. The PBS is used for postselection of the polarization qubit, and the spatial-mode states of the same polarization are preserved, while different polarization states are ignored. Hadamard operations are needed to convert the PF noise to BF noise before purification. (d) Quantum state tomography setup. DM, dichroic mirror; QWP, quarter-wave plate.

In our experiment, we added symmetrical BF noise to both the polarization and spatial-mode d.o.f., so that $F_P \approx F_S \approx F$. The BF noise loading setup [26] can add any proportion of BF noise ($|\Psi^+\rangle_{ab}$ and $|\psi^+\rangle_{ab}$) to the hyperentangled state of the polarization and spatial modes. We loaded 20% BF noise into the ideal state, and when it was combined with the MCF, the fidelities of the polarization and spatial-mode states were $F_P^{0.8} = 0.771 \pm 0.002$ and $F_S^{0.8} = 0.771 \pm 0.002$, respectively. When 30% BF noise was added, the fidelities of the polarization and spatial-mode states were $F_P^{0.7} = 0.666 \pm 0.002$ and $F_S^{0.7} = 0.664 \pm 0.002$, respectively.

The purification setup is rather simple and only contains a PBS and a HWP [Fig. 2(c)]. It is essentially the controlled-NOT (CNOT) gate between the polarization and spatial-mode d.o.f. for a single photon. Unlike the CNOT gate between two photons in polarization, such a CNOT gate works in a deterministic way and does not exploit the auxiliary single photon. The control qubit can be regarded as a spatial-mode qubit ($|a_1\rangle = |0\rangle, |a_2\rangle = |1\rangle$), and the target qubit can be regarded as the polarization qubit. The CNOT gate makes $|0\rangle|H\rangle \to |0\rangle|H\rangle$, $|0\rangle|V\rangle \to |0\rangle|V\rangle$, $|1\rangle|H\rangle \to |1\rangle|V\rangle$, and $|1\rangle|V\rangle \to |1\rangle|H\rangle$. After the CNOT operation, the second operation is to postselect the polarization qubit. Through the PBS, the spatial-mode states with the same polarization are retained, and different polarization states are ignored. The purification process is completed. The experimental results show that the fidelity of the purified state was significantly improved for BF noise [Fig. 3(a)]. For 20% BF noise, the fidelity after purification became $F^{0.8} = 0.887 \pm 0.001$, which is very close to the theoretically predicted value $F = 0.896$. For 30% BF noise, the fidelity after purification became $F^{0.7} = 0.774 \pm 0.002$, which is also very close to the theoretical value $F = 0.778$.

BF and PF noise can be converted to each other through the Hadamard operations (see Supplemental Material [26]). We also show that our protocol is still feasible in the case of PF noise. A PF noise proportion of 20% ($|\Phi^-\rangle_{ab}$ and $|\phi^-\rangle_{ab}$) was loaded into the hyperentangled state. When this was combined with the MCF noise, the fidelities of the polarization and spatial-mode states were $F_P^{0.8} = 0.793 \pm 0.002$ and $F_S^{0.8} = 0.796 \pm 0.002$, respectively. Different from the case of BF noise, we first converted PF noise into BF noise through Hadamard operations and then completed entanglement purification. The fidelity after purification is $F^{0.8} = 0.903 \pm 0.001$, which is also very close to the theoretical value $F = 0.932$. For hyperentangled states with only MCF noise, we found that PF noise (~3.3%) was much higher than BF noise (~1.1%). After the purification, the fidelity was $F = 0.974 \pm 0.001$. This is higher than the fidelity of the polarization or spatial-mode state before purification, which shows that our purification was efficient in fiber distribution.

Finally, let us show the practical application of this purification experiment. The first is to increase the secure key rate [36] in entanglement-based QKD [25]. Secure

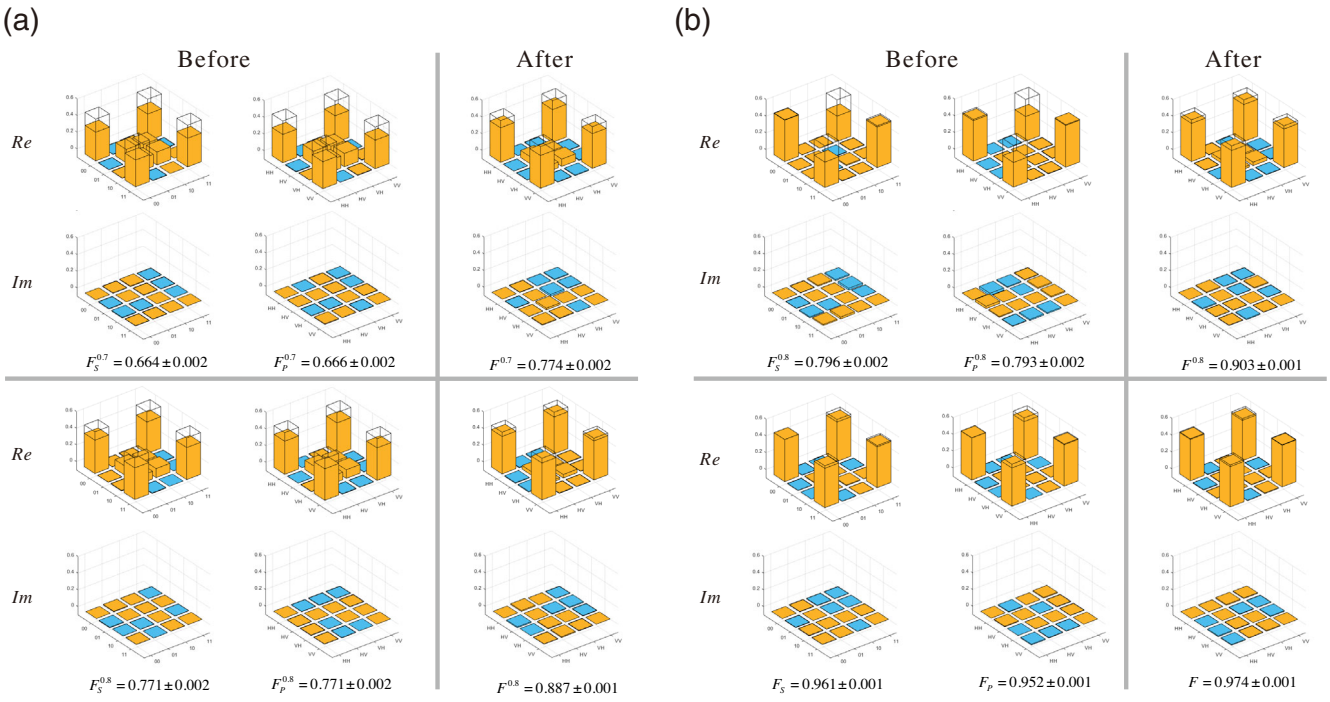

FIG. 3. Experimental results. (a) Results before and after BF noise purification. On the left are the density matrices of polarization and path-entangled states before purification, and on the right are the density matrices of path states after purification. The yellow column represents a value greater than 0, and the blue column represents a value less than 0. The transparent column represents the value of the ideal maximally entangled state. The fidelity of the purified quantum state has obviously been improved significantly. (b) Results before and after PF noise purification. The first half is the result of loading 20% PF noise. The second half is the result of noise introduced only by the MCF.

QKD requires that the quantum bit error rate (QBER) is less than 11% (QBER $= 1 - F$, F is fidelity) [2] to generate an effective key rate (R). In 20% BF noise and 20% PF noise cases, as shown in Figs. 4(a) and 4(b), after purification, the R increases significantly from 0 or nearly 0 to 0.332 ± 0.010 and 0.371 ± 0.009. Here R is defined as $R = 1\text{–}2H(\text{QBER})$, where $H(e)$ represents the Shannon entropy, given as a function of the QBER by $H_e(e) = -(1-e)\log_2(1-e) - e\log_2(e)$. We also show the improvement of R along a real noise channel in Fig. 4(c). The second is to distill nonlocality from nonlocal resources [37], which has the potential application to

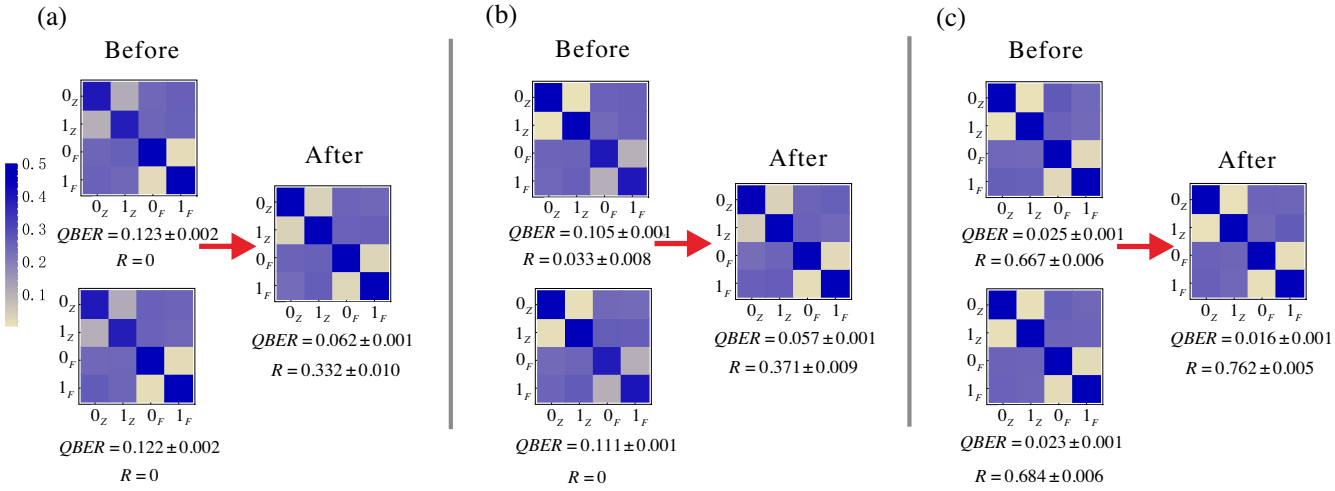

FIG. 4. QKD based on entanglement purification. (a)–(c) The correlations for mutually unbiased bases required for QKD [computational bases ($|0\rangle_Z$, $|1\rangle_Z$) and Fourier bases $|0\rangle_F$, $|1\rangle_F$] before and after purification in the case of loading 20% BF noise, 20% PF noise, and using MCF only. The corresponding QBER and quantum key rate (R) are also presented.

improve the noise tolerance in future device-independent QKD (DI-QKD) [38]. Using the reconstructed density matrix, we can calculate the values of Clauser-Horne-Shimony-Holt inequality of these nonlocal quantum states. Initially, for 30% BF noise, $S_S = 1.837 \pm 0.006 < 2$ for spatial-mode entanglement and $S_P = 1.829 \pm 0.006 < 2$ for polarization entanglement. After purification, $S = 2.128 \pm 0.006 > 2$ (see Supplemental Material [26]).

The integration time of each data point is 60 s, and the count rate of the entangled source after fiber distribution is ~600/s (before purification). After purification, due to the influence of postselection, the successful events are retained and the failure events are ignored, thus the count rate of the entangled source after purification is reduced, respectively. For 30% BF noise, the count rate of purified entangled source is ~350/s; for 20% BF and PF noise, the count rate of purified entangled source is ~410/s.

We propose and demonstrate the first long-distance polarization entanglement purification and show its practical application to increase the secure key rate in entanglement-based QKD and improve the noise tolerance in DI-QKD. Compared with all two-copy EPPs based on Ref. [7], our EPP using one pair of hyperentanglements has several advantages. First, this protocol reduces half of the consumption of copies of entangled pairs. Second, benefited from the success probability 100% CNOT gate between the polarization and spatial inner d.o.f., the purification efficiency of this EPP is 4 times than that of two-copy EPPs in Refs. [8,10,26]. Third, if we consider the experimental implementation (SPDC sources), the double-pair emission noise in generating two clean pairs can be removed automatically and the purification efficiency can be estimated as 1.65×10^3 times than the EPPs using two pairs entangled states with SPDC sources. The total purification efficiency can be calculated as $4 \times 1.65 \times 10^3 = 6.6 \times 10^3$ than the EPPs using two pairs entangled states with SPDC sources. It is worth noting that, since both outcomes of PBSs are used for postselection, we need two sets of measurement setups at both sides of Alice and Bob. However, in the two-copy EPPs [10], two photons act as triggers, so two additional measurement setups are also needed. Our protocol is general and can be effectively extended to other d.o.f. of photons, such as the time bin [39], frequency [40], and orbital angular momentum [18], to perform multistep purification to improve the fidelity of entanglement further. Moreover, if combining with the suitable high-capacity and high-fidelity quantum memory [41] and entanglement swapping [18,42], the approach presented here could be extended to implement the full repeater protocol and large-scale quantum networks, enabling a polynomial scaling of the communication rate with distance.

This work was supported by the National Key Research and Development Program of China (Grants No. 2017YFA0304100, No. 2016YFA0301300, and No. 2016YFA0301700), National Natural Science Foundation of China (Grants No. 11774335, No. 11734015, No. 11874345, No. 11821404, No. 11904357, No. 11974189), the Key Research Program of Frontier Sciences, CAS (Grant No. QYZDY-SSW-SLH003), Science Foundation of the CAS (ZDRW-XH-2019-1), the Fundamental Research Funds for the Central Universities, Science and Technological Fund of Anhui Province for Outstanding Youth (2008085J02), Anhui Initiative in Quantum Information Technologies (Grants No. AHY020100 and No. AHY060300).

*shengyb@njupt.edu.cn
†bhliu@ustc.edu.cn
‡cfli@ustc.edu.cn

[1] R. Horodecki, P. Horodecki, M. Horodecki, and K. Horodecki, Rev. Mod. Phys. **81**, 865 (2009).
[2] V. Scarani, H. Bechmann-Pasquinucci, N. J. Cerf, M. Dušek, N. Lütkenhaus, and M. Peev, Rev. Mod. Phys. **81**, 1301 (2009).
[3] S. Pirandola, J. Eisert, C. Weedbrook, A. Furusawa, and S. L. Braunstein, Nat. Photonics **9**, 641 (2015).
[4] Y. Guo, B.-H. Liu, C.-F. Li, and G.-C. Guo, Adv. Quantum Technol. **2**, 1900011 (2019).
[5] G. L. Long and X. S. Liu, Phys. Rev. A **65**, 032302 (2002).
[6] H. J. Kimble, Nature (London) **453**, 1023 (2008).
[7] C. H. Bennett, G. Brassard, S. Popescu, B. Schumacher, J. A. Smolin, and W. K. Wootters, Phys. Rev. Lett. **76**, 722 (1996).
[8] J.-W. Pan, C. Simon, C. Brukner, and A. Zeilinger, Nature (London) **410**, 1067 (2001).
[9] H. J. Briegel, W. Dür, J. I. Cirac, and P. Zoller, Phys. Rev. Lett. **81**, 5932 (1998).
[10] J.-W. Pan, S. Gasparoni, R. Ursin, G. Weihs, and A. Zeilinger, Nature (London) **423**, 417 (2003).
[11] L.-K. Chen, H.-L. Yong, P. Xu, X.-C. Yao, T. Xiang, Z.-D. Li, C. Liu, H. Lu, N.-L. Liu, L. Li *et al.*, Nat. Photonics **11**, 695 (2017).
[12] R. Reichle, D. Leibfried, E. Knill, J. Britton, R. B. Blakestad, J. D. Jost, C. Langer, R. Ozeri, S. Seidelin, and D. J. Wineland, Nature (London) **443**, 838 (2006).
[13] N. Kalb, A. A. Reiserer, P. C. Humphreys, J. J. W. Bakermans, S. J. Kamerling, N. H. Nickerson, S. C. Benjamin, D. J. Twitchen, M. Markham, and R. Hanson, Science **356**, 928 (2017).
[14] J. T. Barreiro, N. K. Langford, N. A. Peters, and P. G. Kwiat, Phys. Rev. Lett. **95**, 260501 (2005).
[15] J. T. Barreiro, T. C. Wei, and P. G. Kwiat, Nat. Phys. **4**, 282 (2008).
[16] X.-M. Hu, Y. Guo, B.-H. Liu, Y.-F. Huang, C.-F. Li, and G.-C. Guo, Sci. Adv. **4**, eaat9304 (2018).
[17] Y. B. Sheng, F. G. Deng, and G. L. Long, Phys. Rev. A **82**, 032318 (2010).
[18] X.-L. Wang, X.-D. Cai, Z.-E. Su, M.-C. Chen, D. Wu, L. Li, N.-L. Liu, C.-Y. Lu, and J.-W. Pan, Nature (London) **518**, 516 (2015).
[19] T. M. Graham, H. J. Bernstein, T. C. Wei, M. Junge, and P. G. Kwiat, Nat. Commun. **6**, 7185 (2015).

[20] F. Steinlechner, S. Ecker, M. Fink, B. Liu, J. Bavaresco, M. Huber, T. Scheidl, and R. Ursin, Nat. Commun. **8**, 15971 (2017).
[21] X.-M. Hu, W.-B. Xing, B.-H. Liu, D.-Y. He, H. Cao, Y. Guo, C. Zhang, H. Zhang, Y.-F. Huang, C.-F. Li, and G.-C. Guo, Optica **7**, 2334 (2020).
[22] C. Simon and J. W. Pan, Phys. Rev. Lett. **89**, 257901 (2002).
[23] Y. B. Sheng and F. G. Deng, Phys. Rev. A **82**, 044305 (2010).
[24] X. H. Li, Phys. Rev. A **82**, 044304 (2010).
[25] A. K. Ekert, Phys. Rev. Lett. **67**, 661 (1991).
[26] See Supplemental Material at http://link.aps.org/supplemental/10.1103/PhysRevLett.126.010503 for more details about the experiment, which includes Refs. [27–30].
[27] X.-M. Hu, C. Zhang, B.-H. Liu, Y. Cai, X.-J. Ye, Y. Guo, W.-B. Xing, C.-X. Huang, Y.-F. Huang, C.-F. Li, and G.-C. Guo, Phys. Rev. Lett. **125**, 230501 (2020).
[28] A. Acín, N. Brunner, N. Gisin, S. Massar, S. Pironio, and V. Scarani, Phys. Rev. Lett. **98**, 230501 (2007).
[29] L. Zhou, Y. B. Sheng, and G. L. Long, Sci. Bull. **65**, 12 (2020).
[30] C. Brukner, M. Zukowski, J.-W. Pan, and A. Zeilinger, Phys. Rev. Lett. **92**, 127901 (2004).
[31] T. Kim, M. Fiorentino, and F. N. C. Wong, Phys. Rev. A **73**, 012316 (2006).
[32] Y. Guo, X.-M. Hu, B.-H. Liu, Y.-F. Huang, C.-F. Li, and G.-C. Guo, Phys. Rev. A **97**, 062309 (2018).
[33] G. B. Xavier and G. Lima, Commun. Phys. **3**, 9 (2020).
[34] G. Cañas, N. Vera, J. Cariñe, P. González, J. Cardenas, P. W. R. Connolly, A. Przysiezna, E. S. Gómez, M. Figueroa, G. Vallone *et al.*, Phys. Rev. A **96**, 022317 (2017).
[35] D. Bacco, B. D. Lio, D. Cozzolino, F. D. Ros, X. Guo, Y. Ding, Y. Sasaki, K. Aikawa, S. Miki, H. Terai *et al.*, Commun. Phys. **2**, 140 (2019).
[36] P. W. Shor and J. Preskill, Phys. Rev. Lett. **85**, 441 (2000).
[37] P. Walther, K. J. Resch, C. Brukner, A. M. Steinberg, J. W. Pan, and A. Zeilinger, Phys. Rev. Lett. **94**, 040504 (2005).
[38] E. Y.-Z. Tan, C. C.-W. Lim, and R. Renner, Phys. Rev. Lett. **124**, 020502 (2020).
[39] A. Martin, T. Guerreiro, A. Tiranov, S. Designolle, F. Frowis, N. Brunner, M. Huber, and N. Gisin, Phys. Rev. Lett. **118**, 110501 (2017).
[40] M. Kues, C. Reimer, P. Roztocki, L. R. Cortés, S. Sciara, B. Wetzel, Y. Zhang, A. Cino, S. T. Chu, B. E. Little *et al.*, Nature (London) **546**, 622 (2017).
[41] Y. Yu, F. Ma, X.-Y. Luo, B. Jing, P.-F. Sun, R.-Z. Fang, C.-W. Yang, H. Liu, M.-Y. Zheng, X.-P. Xie *et al.*, Nature (London) **578**, 240 (2020).
[42] M. K. Bhaskar, R. Riedinger, B. Machielse, D. S. Levonian, C. T. Nguyen, E. N. Knall, H. Park, D. Englund, M. Lončar, D. D. Sukachev, and M. D. Lukin, Nature (London) **580**, 60 (2020).